Common Mode Currents in DC Power Routers

Wu, Yang; Shekhar, Aditya; Soeiro, Thiago Batista; Bauer, Pavol

DOI
10.1109/ICDCM50975.2021.9504614

Publication date
2021

Document Version
Accepted author manuscript

Published in
2021 IEEE 4th International Conference on DC Microgrids, ICDCM 2021

Citation (APA)
Wu, Y., Shekhar, A., Soeiro, T. B., & Bauer, P. (2021). Common Mode Currents in DC Power Routers. In *2021 IEEE 4th International Conference on DC Microgrids, ICDCM 2021* (pp. 1-6). Article 9504614 (2021 IEEE 4th International Conference on DC Microgrids, ICDCM 2021). IEEE.
https://doi.org/10.1109/ICDCM50975.2021.9504614

Common Mode Currents in DC Power Routers

Yang Wu, Aditya Shekhar, Thiago Batista Soeiro and Pavol Bauer
Delft University of Technology
email: a.shekhar@tudelft.nl

***Abstract*—The grid reinforcement and energy redirection needs have led to the emergence of Back-To-Back Voltage Source Converter (BTB-VSC) based dc power routers. This paper investigates the low frequency Common Mode Currents (CMCs) that arise in the system if the employed BTB-VSCs have an un-isolated ac path connected in parallel to their output ports. Simulation results are presented to show a sensitivity analysis of lower order harmonics in CMC with respect to the operating active and reactive power of the dc router, dc link voltage, link resistance, modulation method and pole capacitance. Experimental results are shared to show existance of lower order CMC in 3-wire ac link operating in parallel with the dc power router and these are mitigated using zero sequence controller.**

I. Introduction

A. Background on DC Power Routers

The medium and low voltage distribution grids are predominantly ac today. BTB-VSC based power routers can be used for redirecting energy from one point in the ac grid to another [1]–[6]. An illustration of such a power router is shown in Fig. 1.

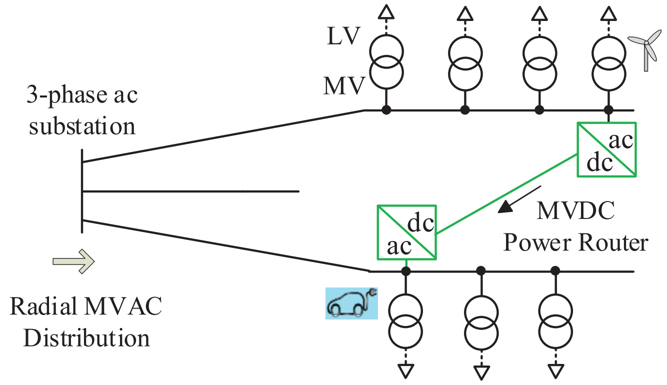

Fig. 1: Meshing the radial ac distribution grids for power redirection using BTB-VSC based dc power router.

In our previous work [7], [8], it was suggested that refurbishing existing ac links for dc operation can increase the power transfer capacity by about 50-60 %. Introducing reconfigurability and modularity in such hybrid ac-dc systems can further improve the grid capacity by 1.5 to 2 times during (n-1) contingencies [9]–[11]. The research study considered data adapted from an actual 10 kV distribution network in The Netherlands. The developed ideas on viability of dc power routing are applicable for medium voltage distribution grids between 10-66 kV few tens of kilometers long and transfering power in the range on few MWs [4]. This application was further extended for optimal placement of embedded DC links in a 33-node IEEE test grid based on efficiency considerations [12].

B. Zero Sequence Current in Hybrid AC-DC Grids

Zero sequence currents can circulate in systems where the BTB-VSC are interconnected at both dc and ac sides without galvanic isolation [13]–[16]. While Common Mode Currents (CMCs) have been investigated in parallel operating converters [17]–[19], the problem is more prominent with BTB-VSC because the difference in terminal ac voltages between the two converters is higher in this case due to the difference in their output power directions. Furthermore, unlike parallel converters where Point of Common Coupling (PCC) is localized at the ac side, the PCC1 and PCC2 can be separated by a large distance, thus CMCs can impact a more significant part of the grid as a consequence. In our previous work [15] it was shown that low frequency Zero Sequence Currents circulate between back-to-back modular multilevel converters operating in parallel ac-dc link systems. Simulation results suggested that ZSC can be reduced with higher submodule capacitance and arm inductance. It was discussed that the ZSC can lead to greater losses particularly for short link lengths within 10 km because the impedance of such parallel ac-dc system is relatively low. A zero sequence controller was simulated to theoretically show that these currents can be successfully mitigated. The focus of the current paper is to present experimental results using 2-level BTB-VSC operating in similar parallel ac dc systems.

C. Research Contributions

The main contribution of this paper is to investigate the magnitude dependence of the lower order harmonics in CMC with respect to operating active and reactive power of the BTB-VSC based dc power router. Several simulation results are presented to understand the variation in CMC with modulation method, dc link voltage, resistance and the pole capacitance. Experimental tests show that lower order CMC exist in 3-wire ac link operating in parallel with the dc power router and a control method to mitigate these CMCs is used.

Section II discussed the theory behind CMC in DC power routers operating in parallel ac-dc link systems. The system description is presented and simulation results for different operating powers are shown. The experimental validation is presented in Section III, while some concluding remarks are made in Section IV.

II. THEORETICAL DISCUSSION

A. System Description

A simulation model is developed corresponding to the system shown in Fig. 2.

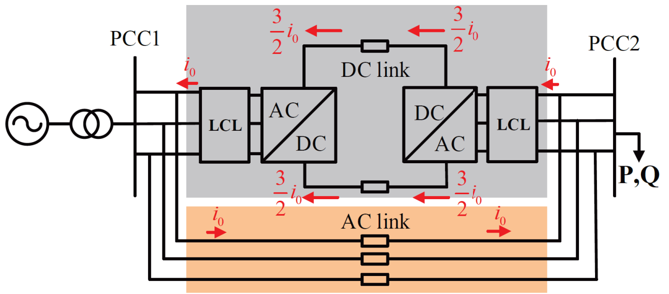

Fig. 2: Common mode currents in a 3-wire ac link operating in parallel with back-to-back voltage source converter based dc links.

While the presented results in both simulation and experimental setup are at low voltage with ac grid phase voltage at PCC is 230 V (rms), the concept is applicable for medium voltage and high power levels as well. The low frequency common mode currents in such systems exist in both two level and multilevel VSC topologies.

A resistive load is connected at PCC 2 with 5 kW power rating. The ac and dc link conductors between the PCC 1&2 are represented with 0.5 Ω and the inductance in the path is neglected assuming a short link length as compared to the filter inductance used. The power router is capable of transferring an active power of $P_{\text{dc,rated}} = 5\,\text{kW}$ between PCC 1& 2 using 2-level ac/dc BTB VSCs operating at 16 kHz switching frequency. With dc link operating at 800 V, sinusoidal modulation technique is used without third harmonic injection. The output ac terminal of the ac/dc VSCs is connected to the PCCs via a LCL filter. The filter inductor and capacitor are rated at 1.5 mH and 20 μF respectively. The topology of the power router is such that it is not electrically isolated from the parallel 3-line ac path that exists between the PCC 1&2. The CMC (i_0) is given by (1),

$$i_0 = \frac{i_{\text{a}} + i_{\text{b}} + i_{\text{c}}}{3} \tag{1}$$

where, i_{a}, i_{b} and i_{c} are the line currents in the parallel ac link.

B. Simulation Results

The dc router is used to steer power P_{dc} in the parallel ac-dc system, given by (2)

$$P_{\text{dc}} + P_{\text{ac}} = P_{\text{load}} \tag{2}$$

Here, P_{ac} is the active power in the parallel ac link and P_{load} is the active load power at PCC2. The dc router power is simulated from 0.5 kW to its rated value for a constant load power of 5 kW at PCC2 as shown in Fig. 3.

The arising CMCs for 1 kW and 4 kW dc link power during steady state is shown in Fig. 4.

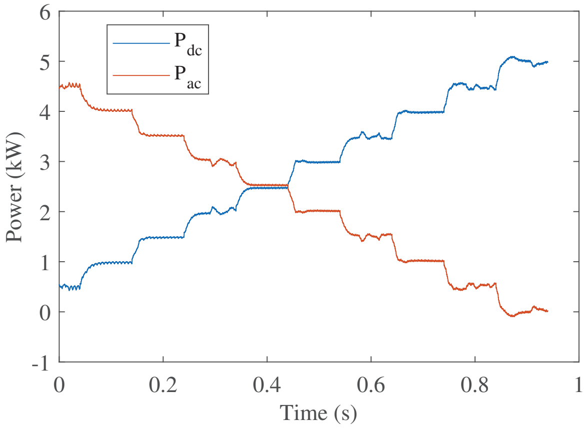

Fig. 3: Active power flow in the dc power router and the parallel ac link while supplying a 5 kW load connected at PCC2.

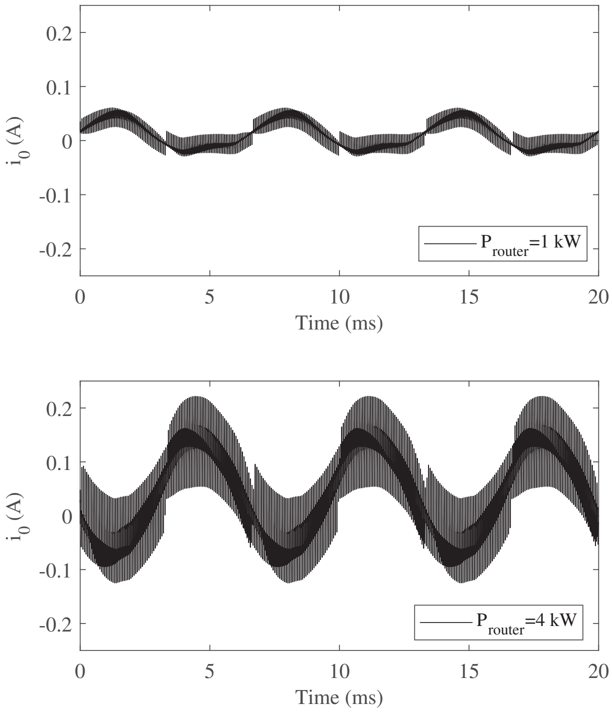

Fig. 4: Common mode currents in a 3-wire ac link operating in parallel with back-to-back voltage source converter based dc links.

It can be observed that the magnitude of third harmonic as well as high frequency component of the CMC increases with operating power level of the router. It should be noted that sinusoidal reference signal with no third harmonic injection is used for this simulation. It is highlighted in [20] that low frequency harmonics can arise due to regularly sampled sinusoidal sawtooth and triangular pulse width modulation unlike the naturally sampled situation. In the subsequent section, the simulated sensitivity analysis of these low frequency CMCs is presented for different operational conditions.

C. Harmonic Analysis

In Fig. 5, the lower order CMCs are shown for different active power levels of the dc router operating in parallel with the ac link to supply the constant $P_{load} = 5\,\text{kW}$ connected at PCC2. The presented analysis is for currents when system reaches steady state for the corresponding operating power. The dc link voltage is 800 V and each link conductor has an resistance of $0.5\,\Omega$. Sinusodal sawtooth modulation is used between ± 1.

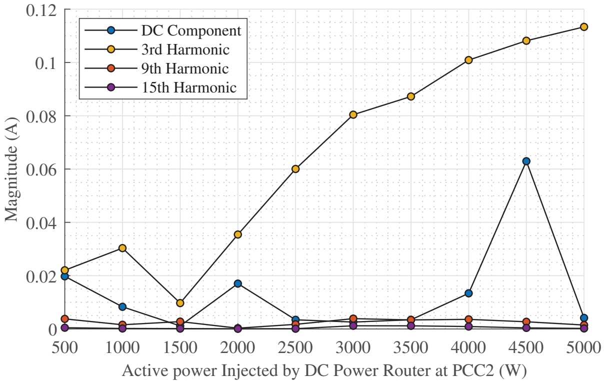

Fig. 5: Lower order harmonics in common mode current with sawtooth modulation at 800 V dc link voltage.

The observed dependence on operating active power is consistent with the study in [21]. In the paper it is suggested that difference between phase (δ_1) and magnitude (ΔV_1) of the fundamental component of the terminal voltage of parallel inverters can increase the CMC circulating in the shared dc bus. Similar simulations are performed for sinusoidal triangular modulation as shown Fig. 6.

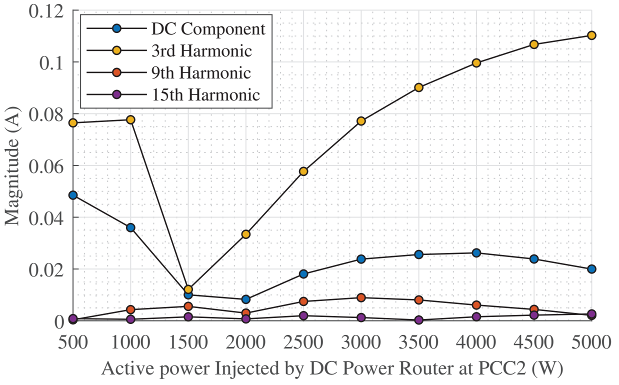

Fig. 6: Lower order harmonics in common mode current with triangular modulation at 800 V dc link voltage.

It can be observed that except for dc power levels below 1 kW, the magnitude of CMC, in particular the third harmonic component is similar to the case with sawtooth PWM. This observation is different from the suggestion in [20], where third harmonic component is expected lower with regularly sampled sinusoidal triagular as compared to the one with sawtooth PWM. However, the study considers only one single phase converter for the presented theory.

Fig. 7 shows the simulation results with dc link voltage reduced from 800 V to 750 V.

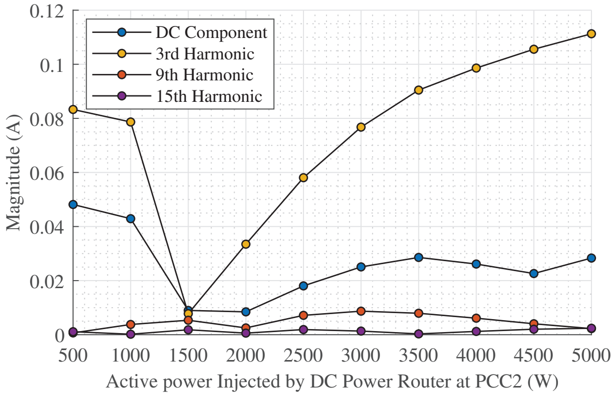

Fig. 7: Lower order harmonics in common mode current with sinusoidal triangular modulation at 750 V dc link voltage.

The lower order CMCs are not significantly different from previous case, indicating limited dependence on the modulation index for these operating conditions. In [21] it is highlighted that the total rms CMC has dependence on modulation index in relation to the phase difference of the fundamental component of the converter terminal voltages. For example, it is shown in [21] that i_0 remains flat and slightly increases when $\delta_1 = 3\,\text{deg.}$ but reduces with $\delta_1 = 6$ deg between parallel operating inverters. Further investigation for validation of these relationships from the context of dc power router is necessary.

In Fig. 8, the lower order CMCs in relation to operating power are shown with each ac and dc link conductor resistance reduced from $0.5\,\Omega$ to $50\,\text{m}\Omega$.

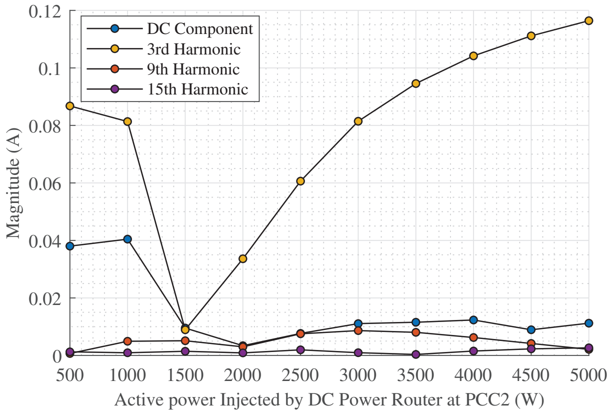

Fig. 8: Lower order harmonics in common mode current with sinusoidal triangular modulation at 800 V dc link voltage and link conductor resistance reduced from $0.5\,\Omega$ to $50\,\text{m}\Omega$.

While the impedance of the circulation path reduces in the considered case, the corresponding increase in CMC is not observed. This is because the link impedance can influence the δ_1 and ΔV_1 between PCC1 and PCC2 for given power levels, such that a reduction in these values can counteract the influence of decreasing path impedance.

Fig. 9 shows the lower order harmonics in CMC with increasing reactive power exchanged by the dc router at PCC1. The active power of the router is fixed at 3 kW operating at 800 V dc link voltage, 50 mΩ link resistances and a constant active load power of 5 kW at PCC2. Again, sinusoidal triangular modulation without thrid harmonic injection is used.

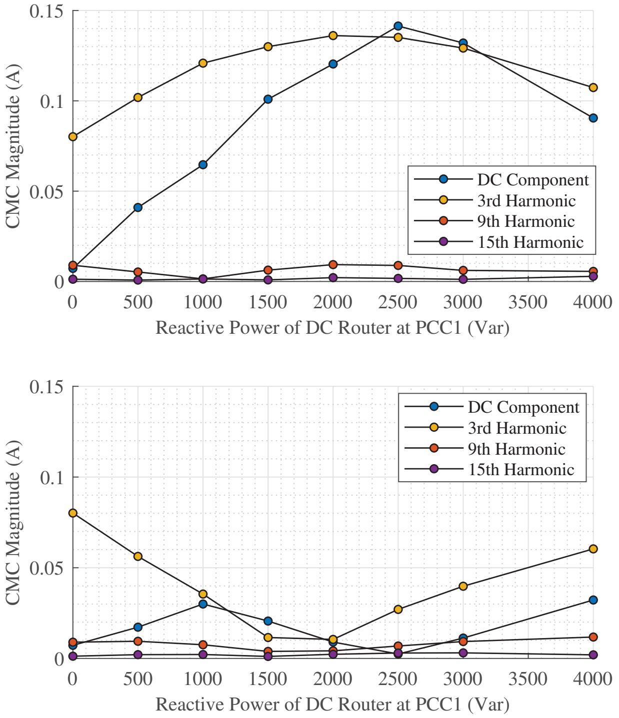

Fig. 9: Lower order harmonics in common mode current with different reactive power at PCC1 with dc router active power at 3 kW (a) injected (b) absorbed.

It can be observed from Fig. 9 (a) that as the reactive power injected from VSC1 to PCC1 is increased from 0 upto 2000 Var, the CMC. On the other hand, it decreases when reactive power is absorbed in Fig. 9 (b). The trend reverses as reactive power is futher increased in either case. This more clearly indicates the dependence on δ_1 and ΔV_1 of the output terminal voltage of the converters because change in reactive power does not change the impedance of the zero sequence path.

Fig. 10 shows the CMCs with increasing active power level when pole capacitance of the dc router is reduced from 600 μF to 300 μF.

The lower order harmonic magnitudes are similar because the considered pole capacitances of the simulated 2-level converters are not in the path of the CMCs, unlike the case with submodule capacitance of modular multilevel converters considered in [15].

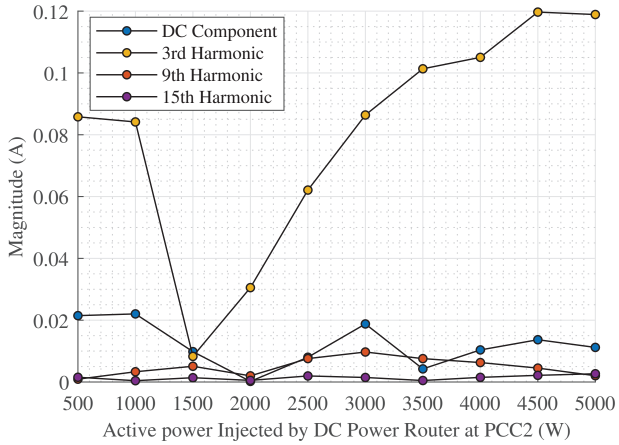

Fig. 10: Lower order harmonics in common mode current with triangular modulation at 800 V dc link voltage and link conductor resistance 50 mΩ with dc pole capacitance reduced from 600 μF to 300 μF.

III. EXPERIMENTAL RESULTS

The experimental setup for BTB-VSC based power router operating in parallel with a 3-line ac link is shown in Fig. 11.

The sending end VSC at PCC1 controls the dc link voltage at 750 V while the VSC at PCC2 controls the active and reactive output of the dc power router. A resistive load of 50 Ω is connected at PCC2. The depicted oscilloscope measures the output ac current of the VSC at PCC2 ($i_{\text{vsc,PCC2}}$), the line current of the parallel 3-wire ac link (i_{ac}) and the dc link current (i_{dc}). The output power of the router is 2.5 kW, such that the entire resistive load power is delivered by the dc link, and therefore the current in the parallel ac system is theoretically zero. A scope screenshot measurement for this operating condition is shown in Fig.12 for waveforms both with and without common mode current controller (CMCC).

The third harmonic component of the zero sequence current is clearly visible in the ac link current (iac=i0/3) and the return path is via the dc link (idc,0=3*i0/2). When the CMCC is activated, these currents are successfully attenuated as shown in the Fig.12.

IV. CONCLUSIONS AND FUTURE WORK

Preliminary results indicate the existence of common mode currents that circulate between the BTB-VSC based dc power router and the 3-wire ac system in parallel. It is shown that the magnitude of these CMCs increase with the operating power of the dc router. A sensitivity analysis with different parameters such as PWM type, dc link voltage, link resistance and pole capacitance is carried out. Experimental results are shared and it is shown that a zero sequence controller can mitigate the existing low frequency CMCs in the dc power router.

As future work, influence of different PWM techniques can be explored to develop a mathematical understanding on the source of the observed CMCs. This mathematical model can include the dependence of CMCs on the fundamental component of phase and magnitude of converter terminal voltage

Fig. 11: Experimental set-up to study the CMC in parallel operating ac and dc links.

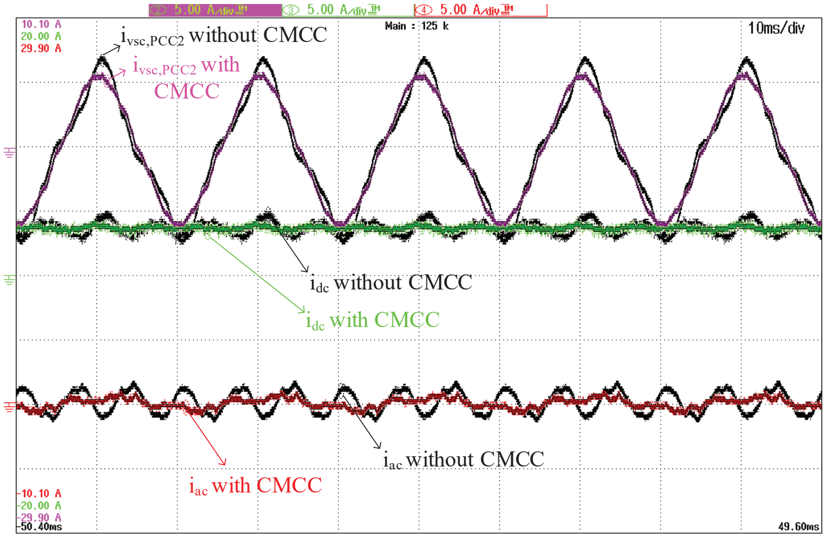

Fig. 12: Experimental demonstration and mitigation of CMC in parallel ac-dc links.

that is influenced by the operating active and reactive powers of the BTB-VSC based dc power routers, corresponding filter impedance, dc link voltage and the interconnecting link impedance. The research topic is relevant because in future, such non-isolated dc power routers operating in parallel with ac links may become increasingly common in the emerging hybrid ac-dc low and medium voltage distribution networks.

REFERENCES

[1] A. Shekhar, L. Ramírez-Elizondo, X. Feng, E. Kontos, and P. Bauer, "Reconfigurable dc links for restructuring existing medium voltage ac distribution grids," *Electric Power Components and Systems*, vol. 45, no. 16, pp. 1739–1746, 2017.

[2] T. Zhang, G. Yao, L. Zhou, N. Jin, J. Cao, J. Hu, and C. Hao, "A novel power router with general ac and dc port," in *2019 IEEE Applied Power Electronics Conference and Exposition (APEC)*, 2019, pp. 3159–3163.

[3] H. Guo, F. Wang, J. Luo, and L. Zhang, "Review of energy routers applied for the energy internet integrating renewable energy," in *2016 IEEE 8th International Power Electronics and Motion Control Conference (IPEMC-ECCE Asia)*, 2016, pp. 1997–2003.

[4] A. Shekhar, L. Ramírez-Elizondo, T. B. Soeiro, and P. Bauer, "Boundaries of operation for refurbished parallel ac–dc reconfigurable links in distribution grids," *IEEE Transactions on Power Delivery*, vol. 35, no. 2, pp. 549–559, 2020.

[5] Y. Zhang, J. Umuhoza, Y. Liu, C. Farnell, H. A. Mantooth, and R. Dougal, "Optimized control of isolated residential power router for photovoltaic applications," in *2014 IEEE Energy Conversion Congress and Exposition (ECCE)*, 2014, pp. 53–59.

[6] J. Miao, N. Zhang, C. Kang, J. Wang, Y. Wang, and Q. Xia, "Steady-state power flow model of energy router embedded ac network and its application in optimizing power system operation," *IEEE Transactions on Smart Grid*, vol. 9, no. 5, pp. 4828–4837, 2018.

[7] A. Shekhar, E. Kontos, A. R. Mor, L. Ramírez-Elizondo, and P. Bauer, "Refurbishing existing mvac distribution cables to operate under dc conditions," in *2016 IEEE International Power Electronics and Motion Control Conference (PEMC)*. IEEE, 2016, pp. 450–455.

[8] A. Shekhar, E. Kontos, L. Ramirez-Elizondo, A. Rodrigo-Mor, and P. Bauer, “Grid capacity and efficiency enhancement by operating medium voltage ac cables as dc links with modular multilevel converters,” *International Journal of Electrical Power & Energy Systems*, vol. 93, pp. 479–493, 2017.

[9] A. Shekhar, E. Kontos, L. Ramírez-Elizondo, and P. Bauer, “Ac distribution grid reconfiguration using flexible dc link architecture for increasing power delivery capacity during (n-1) contingency,” in *2017 IEEE Southern Power Electronics Conference (SPEC)*. IEEE, 2017, pp. 1–6.

[10] A. Shekhar, L. Ramírez-Elizondo, and P. Bauer, “Reliability, efficiency and cost trade-offs for medium voltage distribution network expansion using refurbished ac-dc reconfigurable links,” in *2018 International Symposium on Power Electronics, Electrical Drives, Automation and Motion (SPEEDAM)*. IEEE, 2018, pp. 242–247.

[11] A. Shekhar, T. B. Soeiro, L. Ramírez-Elizondo, and P. Bauer, “Offline reconfigurability based substation converter sizing for hybrid ac–dc distribution links,” *IEEE Transactions on Power Delivery*, vol. 35, no. 5, pp. 2342–2352, 2020.

[12] A. Shekhar, T. B. Soeiro, L. Ramırez-Elizondo, and P. Bauer, “Weakly meshing the radial distribution networks with power electronic based flexible dc interlinks,” *ICDCM 2019*, 2019.

[13] Y. Li, X. Yang, W. Chen, and F. Zhang, “Research on zero-sequence circulating currents in parallel three-level grid-tied photovoltaic inverters,” in *2016 IEEE Energy Conversion Congress and Exposition (ECCE)*, 2016, pp. 1–6.

[14] B. Wei, J. M. Guerrero, J. C. Vásquez, and X. Guo, “A circulating current suppression method for parallel connected voltage-source-inverters (vsi) with common dc and ac buses,” in *2016 IEEE Energy Conversion Congress and Exposition (ECCE)*, 2016, pp. 1–6.

[15] A. Shekhar, T. B. Soeiro, L. Ramírez-Elizondo, and P. Bauer, “Zero sequence currents externally circulating between the back to back modular multilevel converters in parallel ac-dc distribution links,” in *2019 10th International Conference on Power Electronics and ECCE Asia (ICPE 2019 - ECCE Asia)*, 2019, pp. 837–842.

[16] Y. Wu, A. Shekhar, T. B. Soeiro, and P. Bauer, “Voltage source converter control under distorted grid voltage for hybrid ac-dc distribution links,” in *IECON 2019 - 45th Annual Conference of the IEEE Industrial Electronics Society*, vol. 1, 2019, pp. 5694–5699.

[17] J. S. Siva Prasad and G. Narayanan, “Minimization of grid current distortion in parallel-connected converters through carrier interleaving,” *IEEE Transactions on Industrial Electronics*, vol. 61, no. 1, pp. 76–91, 2014.

[18] D. Jiang, Z. Shen, and F. Wang, “Common-mode voltage reduction for paralleled inverters,” *IEEE Transactions on Power Electronics*, vol. 33, no. 5, pp. 3961–3974, 2018.

[19] M. H. Ravanji, N. Amouzegar Ashtiani, M. Parniani, and H. Mokhtari, “Modeling and control of zero-sequence circulating current in parallel converters with space vector modulation,” *IEEE Journal of Emerging and Selected Topics in Power Electronics*, vol. 5, no. 1, pp. 363–377, 2017.

[20] D. G. Holmes and T. A. Lipo, *Modulation of One Inverter Phase Leg*, 2003, pp. 95–153.

[21] T.-P. Chen, “Dual-modulator compensation technique for parallel inverters using space-vector modulation,” *IEEE Transactions on Industrial Electronics*, vol. 56, no. 8, pp. 3004–3012, 2009.